

A photon correlation spectroscopy study of size distributions of casein micelle suspensions

D. S. Horne and D. G. Dalgleish

The Hannah Research Institute, Ayr, Scotland, KA6 5HL

Received July 2, 1984/Accepted December 14, 1984

Abstract. Due to mathematical ill-conditioning there exists a lack of confidence in the uniqueness of the solutions derived by the application of Laplace inversion techniques to photon correlation spectra. Criteria based on the use of multi-angle measurements of the diffusion coefficient are suggested for narrowing the range in the multitude of permitted solutions. Although some results on calibrated, monodisperse latices are included the method is mainly employed to calculate size distributions for casein micelle suspensions providing a 'real' system evaluation of the recently developed exponential sampling technique of Pike and Ostrowsky (Ostrowsky et al. (1981) *Optica Acta* 28: 1059–1070). Notwithstanding the use of exponential sampling software (POLY-BAS) here, the criteria apply equally well to solutions generated using the CONTIN procedure of Provencher [Provencher (1979) *Makromol. Chem.* 180: 201–209].

Key words: Photon correlation spectroscopy, size distributions, casein micelles, Laplace inversion, exponential sampling

1. Introduction

Casein micelles are the roughly spherical aggregates of casein phosphoproteins and calcium phosphate found in milk. They are extremely polydisperse, ranging in diameter from 50 to 600 nm with an average diameter of around 200 nm. Many systems of biological interest exhibit polydisperse properties but few show such extreme range in size within a single sample.

Photon correlation spectroscopy (PCS) allows us to measure the translational diffusion coefficient, D , of structureless, monodisperse particles with great accuracy and ease (Cummins and Pike 1974). For a polydisperse system, the method of cumulants (Pusey

et al. 1974) provides an extremely powerful method of determining the average particle size in solution. Often, however, the main purpose of the experiment is the extraction of the particle size distribution and in this instance the basic problem amounts to inverting the equation

$$g(\tau) = \int_0^{\infty} G(\Gamma) \exp(-\Gamma\tau) d\Gamma \quad (1)$$

in order to derive the linewidth distribution function $G(\Gamma)$ from the measured electric field correlation function $g(\tau)$. Γ is equal to the product of the translational diffusion coefficient of the particle and the square of the scattering wave vector, $k \{= 4\pi n \sin(\theta/2)/\lambda_0$ with n , θ and λ_0 being the refractive index, scattering angle and the wavelength of light in vacuo, respectively}.

A number of methods have attempted to deal with such an integral spectrum. The different approaches may be classified into two main groups:

(i) the empirical methods which include the cumulants expansion (Pusey et al. 1974), the use of parameterized distributions and the more recent histogram decomposition (Gulari et al. 1979).

(ii) the Laplace transform techniques which attempt to tackle the ill-conditioned nature of the problem.

Two computer packages are available in the latter grouping, the program CONTIN by Provencher (1979) using regularization constraint techniques and the commercially available program POLY-BAS used in this study. Based on the "exponential sampling" concept of Pike, Ostrowsky and co-workers (Ostrowsky et al. 1981; Bertero and Pike 1983; Pike et al. 1983), this is now incorporated into software developed for the Malvern K7027 'Log-Lin' correlator.

Generally, ill-conditioning is thought of in terms of the instability of the solution, a small deviation in $g(\tau)$, due to noise for example, leading to large distortions in the recovered $G(\Gamma)$ function. Another facet of the ill-conditioning problem, however, is the non-uniqueness of the solution with a generally infinite set, Ω , of possible solutions satisfying the input data to within experimental error. Both CONTIN and POLY-BAS attempt to tackle this problem of non-uniqueness. Both rely on the acceptance of basic physical truths, eliminating those solutions which predict negative mass or number. CONTIN thereafter invokes a parsimony principle which states that, of all members of Ω that have not been eliminated by prior knowledge, take the 'simplest' solution, i.e., the one that reveals the least amount of new information. In PCS 'simplest' generally means 'smoothest' and CONTIN imposes a bias against the occurrence of peaks and shoulders.

POLY-BAS approaches the problem from a different viewpoint; band-limiting the range of Γ considered, preferably from a priori knowledge, and seeking the solution which provides the maximum resolution in the $G(\Gamma)$ distribution. It has been shown that this resolution limit is a function only of the ratio γ of the upper and lower bounds of the Γ range and of the signal-to-noise ratio in the input data (Bertero and Pike 1983; Pike et al. 1983). Beyond computation of an RMS error comparing output with the input correlogram and an estimation of correlation in these errors, POLY-BAS makes no further assessment of the reliability of this 'maximum resolution' fit.

This paper extends the application of the Laplace transform techniques away from systems where the particles are small compared to the wavelength of the incident light e.g., phospholipid vesicles (Stelzer et al. 1983). The accuracy of the POLY-BAS inversion package is first of all demonstrated using monodisperse polystyrene latices. The bulk of the paper is, however, concerned with its application to 'real' systems which are not monodisperse and which fall in the size range of Rayleigh-Gans-Debye theory, namely suspensions of casein micelles. Using such data, criteria are proposed for establishing confidence in the validity of the final solution. The minimum requirement is that the diffusion coefficient predicted by the proposed size distribution should lie within the error limits of the experimental value at that measuring angle. A more stringent restriction on the solution is that it should further predict an angular variation in this diffusion coefficient comparable to the observed variation. Though the chosen Laplace inversion technique is the exponential sampling one of Pike et al. (1983), it should be stressed that the proposed criteria are equally applicable to solutions

generated via the CONTIN procedure (Provencher 1979).

2. Theoretical background

It was shown by McWhirter and Pike (1978) that the function $G(\Gamma)$ may be expressed in terms of the eigenfunctions and eigenvalues of its Laplace transform as

$$G(\Gamma) = \int_{-\infty}^{\infty} \Psi_{\omega}(\Gamma) a_{\omega} d\omega \quad (2)$$

which yields for $g(\tau)$

$$g(\tau) = \int_{-\infty}^{\infty} \lambda_{\omega} a_{\omega} \Psi_{\omega}(\tau) d\omega \quad (3)$$

with

$$\lambda_{\omega} = \frac{\omega}{|\omega|} \sqrt{\frac{\Pi}{\cosh(\Pi \omega)}} \quad (4)$$

As McWhirter and Pike (1978) pointed out, when ω goes to infinity, λ_{ω} tends to zero which means that for large values of ω , say $\omega \geq \omega_{\max}$, the eigenfunctions are "transmitted" so weakly across Eq. (1) that they cannot be distinguished from the noise in the data. Information on $G(\Gamma)$ can thus only be recovered from that part of the data above the noise level. $G(\Gamma)$ is therefore band-limited and becomes the truncated function $\tilde{G}(\Gamma)$

$$\tilde{G}(\Gamma) = \int_{-\omega_{\max}}^{\omega_{\max}} a_{\omega} \Psi_{\omega}(\Gamma) d\omega \quad (5)$$

with ω_{\max} given by $\lambda_{\omega_{\max}} \approx \text{noise}$.

This truncated or filtered distribution function has no high frequency components and contains the most information which can be safely extracted from the experimental data, $g(\tau)$.

Using the explicit expression for $\bar{\Psi}_{\omega}(\Gamma)$ and changing the variable from Γ to $\log \Gamma$, it was shown (Ostrowsky et al. 1981) that

$$\exp\left(-\frac{1}{2} \log \Gamma\right) G(\log \Gamma) = \int_{-\omega_{\max}}^{\omega_{\max}} \beta(\omega) \exp(i\omega \log \Gamma) d\omega \quad (6)$$

The function on the left-hand side is thus a band-limited Fourier transform for which the sampling theorem applies (McWhirter and Pike 1978). The function can therefore be fully reconstructed from knowledge of its values at points $\log \Gamma_n, \log \Gamma_{n+1}$

etc separated by Π/ω_{\max} using the interpolation formula

$$\exp\left(-\frac{1}{2}\log\Gamma\right)G(\log\Gamma) \\ = \sum_{n=1}^{\infty} \exp\left(-\frac{1}{2}\log\Gamma_n\right)G(\log\Gamma_n) \frac{\sin[\omega_{\max}\log(\Gamma/\Gamma_n)]}{\omega_{\max}\log(\Gamma/\Gamma_n)} \quad (7)$$

with $\Gamma_n = \exp\left(\frac{\Pi}{\omega_{\max}}\right) \cdot \Gamma_{n-1}$. In the POLY-BAS software $\exp(\Pi/\omega_{\max})$ is termed the dilatation factor (DF). Ostrowsky et al. (1981) have shown that

$$G(\log\Gamma_n) = \frac{\omega_{\max}}{\Pi} a_n. \quad (8)$$

Thus replacing the true function, $G(\Gamma)$, by its truncated version amounts to fitting the data to

$$g_{\text{th}}(\tau) = \sum_{n=1}^N a_n \exp(-\Gamma_n \tau), \quad (9)$$

where N = no. of sampling points for $G(\Gamma)$.

The coefficients, a_n , are computed by minimizing, over the M experimental points of the correlation function, the sum of squares

$$\sum_{j=1}^M [g_{\text{ex}}(\tau_j) - g_{\text{th}}(\tau_j)]^2.$$

As noted earlier $\Gamma_n = \exp(n\Pi/\omega) \Gamma_0 = \delta_0^n \Gamma_0$, δ_0 being the dilation factor, allowing its use as an input variable in the POLY-BAS procedure. Bertero and Pike (1983) have shown that the resolution limit to this dilation factor is a function not only of the signal-to-noise ratio in the input data but also of the ratio of the upper and lower bounds of the range of Γ . The relationship between the number of coherence times, N_c , in an experiment (effectively the experiment duration) and its noise level, and hence the number of parameters that may be extracted from the data has no exact solution at present. Studies (Pike et al. 1983) indicate that to resolve two points $N_c \approx 10^3$ – 10^4 , to resolve three points, $N_c \approx 10^6$, four points $N_c \approx 10^8$ and so on. These results confirm and quantify what has been known in photon correlation spectroscopy for many years, namely, that in practice one is not able to resolve more than, at best, about three fairly well-spaced components. Attempts to push the resolution beyond these limits or to extract more parameters than are allowed by the considerations outlined generally give rise to oscillatory fits with large negative excursions in the weights assigned to the components and an obviously unphysical result.

The number or weight fraction of particles of each size can be calculated from the computed line-width distribution $G(\Gamma)$ by use of the necessary scattering factor corrections. Most workers regard the conversion of the distribution of decay constants to a distribution of particle sizes as a completely independent problem from the inversion to obtain $G(\Gamma)$ but, as is demonstrated herein, this conversion can play an integral part in demonstrating the uniqueness and assessing the reliability of the derived solution.

Since we are considering dilute suspensions of spherical, rigid particles, the correlation function contains decay time components due solely to the translational motion of the particles. Under these circumstances, if the particles have a number fraction radius distribution $N(R)dR$, the photon correlation spectrum is now the sum of spectra due to each particle weighted by the intensity $I(R, k)$ it scatters in direction θ . The normalized correlation function is thus:

$$g(\tau) = \frac{\int N(R)I(R, k) \exp(-D(R)k^2\tau) dR}{\int N(R)I(R, k) dR}. \quad (10)$$

The correspondence thus exists that

$$G(\Gamma)d\Gamma = N(R)I(R, k) \left(\frac{d\Gamma}{dR}\right) dR \quad (11)$$

so that $N(R)$ can be obtained from a PCS experiment only if $I(R, k)$ is known. For these calculations it is assumed that the particles may be approximated as smooth, homogeneous spheres with mass proportional to the cube of the radius, so that the particle scattering factor is given by (Kerker 1969)

$$P(R, k) = \left[\frac{3}{(kR)^3} \{ \sin(kR) - kR \cos(kR) \} \right]^2. \quad (12)$$

Then $I(R, k)$ is given by

$$I(R, k) = C \cdot R^6 P(R, k), \quad (13)$$

where C is a constant involving the polarizability of the particles and cancelling on normalizing.

The first cumulant of the autocorrelation function yields an apparent diffusion coefficient (Pusey et al. 1974) whose angular dependence is described by the equation

$$D_{z, \text{app}}(k^2) = \frac{\int N_i M_i^2 P(R_i, k) D_i dR_i}{\int N_i M_i^2 P(R_i, k) dR_i}. \quad (14)$$

The suffix z is attached to the diffusion coefficient since $P(R_i, k) \rightarrow 1$ as $k \rightarrow 0$, and, in that limit, this

equation defines a z -average quantity. From this equation it is seen that angular variation in $D_{z,app}$ is detectable only when $P(R_p, k)$ has significant angular variation. Moreover, for a monodisperse system, the scattering factor will cancel and the diffusion coefficient will show no angular variation.

3. Experimental and methods

The photon correlation spectrometer consisted of a scattering photometer with temperature controlled water bath and variable scattering angle turntable, collection optics and photomultiplier tube followed by pulse amplifier and discriminator and a K7027 'LOG-LIN' correlator (Malvern Instruments Ltd., Malvern, Worcs. England). The light source was a Spectra Physics HeNe Laser, Model 124B.

To facilitate subsequent POLY-BAS analysis, the correlator was operated in the logarithmic mode. This provides a means of spacing correlator channels not at adjacent sample times but at intervals separated by a logarithmic or geometric progression. The delayed signal is still stored at all delay times $\Delta T \rightarrow M\Delta T$ where M is now very large ($> 8,000$) but the correlation function is only accumulated in channels at the discrete time points $(\sqrt{2})^k \cdot \Delta T$. In practice, the nearest integer number to the series value is used. The very wide time span of the correlation function and the spacing of the channels in accordance with the distribution of information in the exponential function has been found superior to previous techniques of performing several experiments at a series of sample times and 'splicing' the results together to form a long time span correlogram (Bertero and Pike 1983).

For each scattering angle, correlation data were gathered during many equal consecutive short runs (5–10 s). The final $g(\tau)$ was an average of the results of selected of these separately normalized runs. Runs were included in the average if the difference between the calculated theoretical background and the measured baseline fell below a preselected fraction of the theoretical value. Typically this rejection factor was set at 0.001. Thus data accumulated when the scattering was unduly influenced by 'dust' or other anomalous conditions could be rejected. The use of multiple short runs also minimized the effects of possible fluctuations in the laser intensity.

Polystyrene latices were obtained from Sigma (London) Ltd. The latex solutions were prepared by diluting the original material with a 5-mM NaCl solution which had been previously filtered through cellulose acetate filters of 0.1 μm pore diameter (Millipore). This latex solution was then filtered through a 0.45 μm pore membrane directly into the scattering cell.

Fresh whole milk was obtained from the Hannah Research Institute farm after the morning milking and was skimmed by centrifugation as outlined previously (Horne and Parker 1980). The fat content of the skimmed milk was further depleted by vacuum filtration through glass-fibre filters (Whatman GF/A) followed by pressure filtration through cellulose acetate membrane (Millipore, 0.8 μm pore diameter). Defined fractions of casein micelles were then prepared by successive centrifugation steps using a Sorval RC-2B centrifuge according to the conditions given in Table 1. After each centrifugation, the pellet of sedimented casein micelles was drained and resuspended in milk ultrafiltrate. The supernatant from each centrifugation step was then subjected to a further centrifugation to provide the next pellet of smaller micelles. Occasionally a supernatant was used in the PCS experiments to provide a micellar suspension depleted in larger sized micelles.

Milk ultrafiltrate was prepared in an Amicon TCF10A ultrafiltration system equipped with a Diaflo membrane, type PM30 (Amicon Ltd., Stonehouse, Glos. England). For PCS measurements, 5 μl of milk or resuspended micelles were diluted into 2 ml of a solution of 5 mM CaCl_2 in a buffer of 20 mM imidazole adjusted to pH 7 with HCl. This buffer, which also contained 50 mM NaCl, had previously been filtered through a cellulose membrane filter, pore diameter 0.1 μm . Preliminary measurements of D_z showed that the diffusion coefficient of the micellar suspensions was independent of concentration at the levels used in these experiments. All measurements were made at 20°C.

$G(D)$ rather than $G(t)$ was calculated using the POLY-BAS software supplied by Malvern Instruments for use on their K7027 correlator. Further analysis on the linewidth distributions so derived were made on a DEC 11/23 minicomputer.

4. Results and discussion

A large number of measurements were performed with suspensions of polystyrene latices and with

Table 1. Centrifugation conditions for casein micelle fractionation

Pellet	Rotor speed (rpm)	$g \times 10^{-3}$	Time (min)
1	8,000	10.7	15
2	10,000	16.7	15
3	12,000	24.1	15
4	15,000	37.7	15
5	18,000	54.3	15
6	19,000	60.5	15
7	19,000	60.5	30
8	19,000	60.5	60

suspensions of casein micelles, the latter differing both in average size and width of the size distribution. Except for the suspensions from skim-milk, these micellar suspensions were believed to be unimodal and hence polydisperse rather than heterodisperse as defined by Grabowski and Morrison (1983). No measurements were attempted on mixtures of resuspended micelles i.e., no calculations on deliberately prepared bimodal suspensions were considered in this study.

The following example serves to illustrate the analytical procedure. The input parameters for the POLY-BAS analysis were a lower size limit on the diameter (LS) on which the first contributing delta function is sited, an upper size limit (US) and a dilation factor (DF), the δ_0 defined previously. The upper size limit (US) was used only in limiting the inclusion but not the position of the highest delta function contributing to the fit. The components and their positions were fixed by LS and the geometric progression multiplier, the dilation factor. The fitting was an interactive process initiated by the operator selecting a few delta functions widely spread and then improved by increasing the number of components and decreasing their spacing until the fit became unstable – typical evidence of this being large oscillations between positive and negative values in the weights assigned to the components in the fit.

As already noted, Bertero and Pike (1983) have demonstrated that the limiting value of the dilation factor is a function not only of the noise level in the data but also of the ratio US/LS. Restricting the range of radius values included in the calculation therefore allowed lower values of the dilation factor, and hence greater resolution, to be achieved. The knowledge that each latex solution was practically monodisperse permitted a particularly narrow size range to be used for each. In the case of the smaller latex particles a minimum dilation factor of 1.10 was reached with correlation function data accumulated over 4–5 min. The solution generated included three components and all were given positive weights, the first being sited at 165 nm. Using the interpolation formula of Eq. (7) and assuming particle-scattering factors to be given by Eq. (12), the number fraction curve calculated from this solution is compared in Fig. 1 with a Gaussian number fraction curve calculated from the nominal data supplied by the manufacturer of the latex particles. For these latex particles, with a particularly narrow distribution, acceptable accuracy was achieved for the mean radius, 85.5 nm and standard deviation (S), 5.5 nm as opposed to the 86.5 nm and 1.15 nm specified.

A second example, also shown in Fig. 1, gave an estimate from POLY-BAS inversion of 152.6 nm for the number average radius of the latex particles but a

standard deviation of 12.5 nm. The specifications were a mean radius of 152.5 nm and a standard deviation of 4.5 nm. Only two components were included in the inversion calculation for these larger latex particles and the minimum dilation factor reached was 1.15.

These results clearly indicate that POLY-BAS was very successful in the analysis of the correlation functions from monodisperse latices. The mean radius was always in good agreement with the specifications. In this, the POLY-BAS inversion procedure is comparable to the CONTIN package of Provencher (1979). As has also been found by Ostrowsky and Sornette (1983), the resolution achieved with POLY-BAS is perhaps not as high as that attained with CONTIN, but as demonstrated by Bertero and Pike (1983) the quality of the data is also an important factor dictating the resolution permissible in these inversion procedures.

In these instances of essentially monodisperse model suspensions, the knowledge that the system is monodisperse allows the user of POLY-BAS to restrict the included size range and push the resolution to the limits permitted by the noise level in the data. Real systems are, however, invariably polydisperse and knowledge of the size range is often imperfect. The problems encountered in using POLY-BAS to analyse correlation functions from such systems are illustrated in the following example.

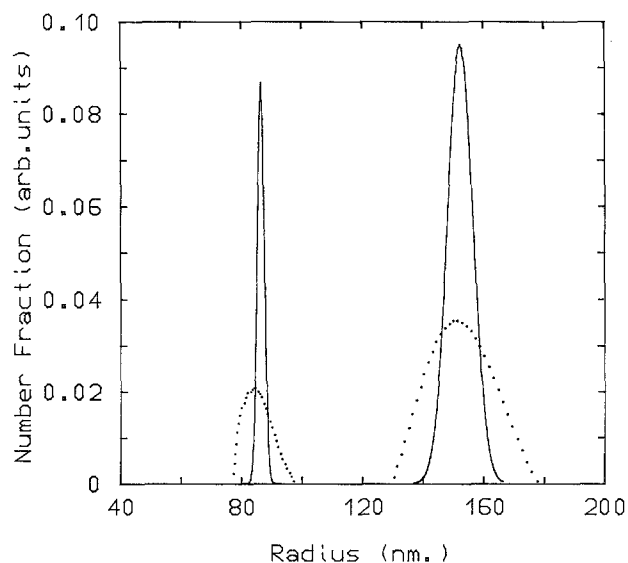


Fig. 1. Comparison of the Gaussian distributions of calibrated latices (solid lines) with the distributions generated by POLY-BAS inversion of their individual correlation functions. The POLY-BAS output has been corrected for particle scattering factor behaviour and computed on a number fraction basis. The mean radii specified for these latices were 86.5 and 152.5 nm. All the distribution functions are normalized to unit area

The starting point for this set of analyses was a single correlation function obtained from a dilute suspension of casein micelles from the supernatant left after the preparation of the second pellet. Cumulant analysis of this correlation function gave a diffusion coefficient of $2.49 \times 10^{-8} \text{ cm}^2 \text{ s}^{-1}$, equivalent to a diameter of 172.4 nm, and a polydispersity of 0.090. Knowing that the undiluted supernatant itself had passed through a cellulose acetate membrane of 0.45 μm pore diameter, the upper size limit could be safely fixed at 450 nm. Varying the lower size limit and the dilation factor in accordance with the general approach it was found that attempts to push the resolution beyond a dilation factor of 1.6 or to incorporate more than three components into the analysis resulted in large negative excursions in the fit.

The maximum resolution having been achieved in this way, the POLY-PAS procedure makes no further attempt to demonstrate the uniqueness of this final distribution or to establish any confidence in its relationship to the true size distribution of the suspended particles. Stepping back from this resolution limit, a series of solutions were generated using different parameter settings close to those used in the maximum resolution fit. All of the solutions generated involved three components, all of these assigned positive weights.

POLY-BAS provided an assessment of the goodness-of-fit by calculating an RMS error between the calculated and measured correlation function and indicated whether these errors varied in a systematic or correlated fashion. For the solutions calculated in this demonstration a low correlation was found, indicating random deviations, together with a low RMS error valued at between 4.7×10^{-4} and 4.8×10^{-4} . Since the experimental error was likely to be in the range of the latter values, it would have been misleading to attempt to calculate a solution converging on a minimum RMS error. Indeed, from a statistical viewpoint, the solutions generated here were indistinguishable from one another, again illustrating the ill-conditioning problem. Some other criteria had to be devised for choosing the 'best-fit' solution.

Using the interpolation formula of Eq. (7), POLY-BAS provided a tabulation of the fit corresponding to the delta functions and their assigned weights. Assuming particle scattering factors given by Eq. (12), it was possible to back-calculate from this exponential weight distribution to the number fraction or weight distribution of the particles and from these calculate, using Eq. (14), the value of the diffusion coefficient at 90° or any other angle. By such calculation, it was possible to demonstrate that for solutions from dilation factors ≤ 1.6 or > 2.0 , the

diffusion coefficients calculated at 90° were of the order of 2.41×10^{-8} (cf. experimental value of 2.49×10^{-8} for this particular correlation function), outside the experimental error. On this basis such solutions were rejected.

The exponential weight distributions given by POLY-BAS for four solutions within the intermediate range (DF from 1.7 to 1.9) are shown in Fig. 2. The peak positions in these $G(R)$ plots were largely unaltered (see also Table 2) and the decreasing dilation factor produced a general narrowing of the peak consistent with its role as controller of resolution. There was some interaction between the input fitting parameters, however, since the distribution with LS = 95 and DF = 1.75 was somewhat narrower than the distribution produced from DF = 1.7 and LS = 85.

Correcting these linewidth distributions for the effects of particle scattering factor and dividing by the

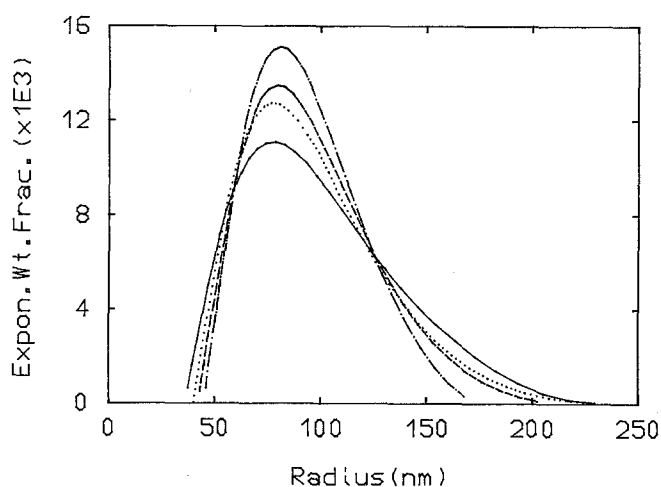


Fig. 2. Exponential weight fraction distributions (POLY-BAS solutions) as a function of particle radius, showing the effect of changing input parameters on the solution derived. All solutions were derived from the same input correlation function. *Solid line* used LS70, DF1.9 and US450; *dotted* LS80, DF1.8, US400; *dashed* LS85, DF1.7, US400; *dashed-dotted* LS95, DF1.75, US400

Table 2. Effect of fitting parameter variation on solutions obtained by inversion of same correlation function. Listed are peak positions for the solutions $[G(R)]$ and the corresponding weight and number fraction distributions derived from $G(R)$. Also given are the diffusion coefficients predicted at 60° and 90° for these size distributions and calculated using Eq. (14)

Fit parameters			Peak position (nm)			$D_{z,app}$ ($\times 10^8 \text{ cm}^2 \text{ sec}^{-1}$)	
LS	US	DF	$G(R)$	$W(R)$	$N(R)$	60°	90°
70	450	1.9	78.5	52.5	44.5	2.04 ₁	2.45 ₁
80	400	1.8	76.5	56.5	49	2.13 ₉	2.47 ₁
85	400	1.7	79	59.5	52	2.22 ₄	2.44 ₉
95	400	1.75	81	65	55	2.33 ₇	2.47 ₇

cube of the particle radius gave the weight fraction distributions of Fig. 3. Further division by R^3 gave the number fraction distributions of Fig. 4. Both number and weight fractions were separately normalized to unity at each stage.

As is apparent in Figs. 3 and 4, the narrowing of the peak in Fig. 2 produced a shift in peak position to higher radius values in both the weight and number fraction distributions. Using these distributions the calculated 90° diffusion coefficients range from 2.44 to 2.47 (Table 2) all within error limit range of the experimentally measured value. It is emphasized, that from a statistical viewpoint, these fits are indistinguishable and yet their weight fraction distributions differed in peak position by more than 12 nm – a less than satisfactory situation.

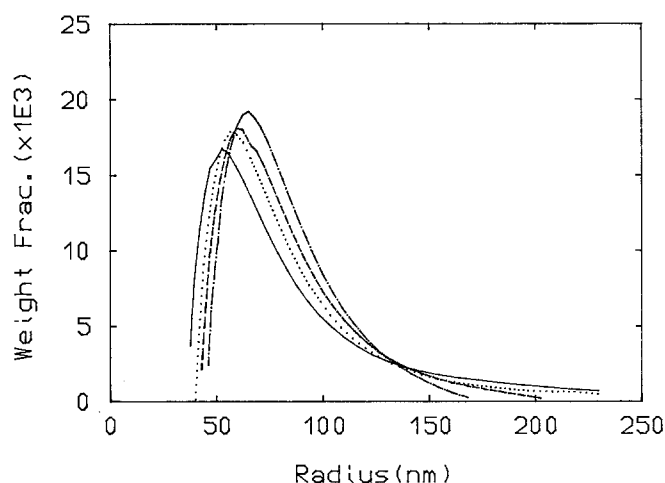


Fig. 3. Weight fraction distributions calculated from the exponential weight fraction distributions of Fig. 2. The same symbols apply

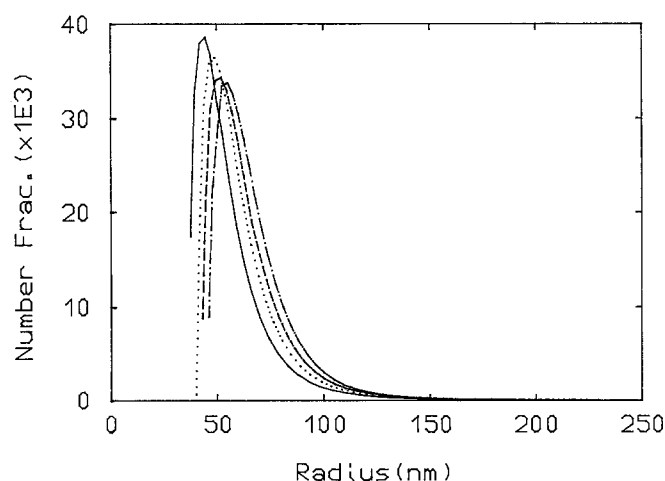


Fig. 4. Number fraction distributions calculated from the exponential weight fraction distributions of Fig. 2. Again the same symbols apply

To assist in further narrowing the choice of 'best-fit' solution we have turned to measurements of the diffusion coefficient as a function of scattering angle. As shown in Fig. 5, the solutions 1–4 predicted a wide spread in angular behaviour for D_z . It is our contention that the 'best-fit' distribution should reproduce the experimentally observed variation of D_z with scattering angle and in this way demonstrate its uniqueness as the final solution. As noted earlier, D_z only shows significant angular variation when this is transmitted through the angular variation of the particle scattering factor. When dealing with monodisperse systems such as our polystyrene latices or with systems of small particles where either $P(\theta)$ cancels or is unchanging with angle, this criterion would be expected to fail. It can, however, be operated in a negative sense and when no angular variation is observed, the final solution should predict no angular variation. In passing we note that the distributions generated from the inverted correlation functions from the latices did give calculated D_z values which showed no angular variation.

These criteria were applied to the solutions inverted by POLY-BAS from autocorrelation functions generated for dilute suspensions of micelles from skim-milk pellets 2, 5, and 7. The experimentally observed angular variations of the diffusion coefficients of these micelles are shown in Fig. 6 together with the predictions of the 'best-fit' POLY-BAS solutions. In this instance calculations were performed only on autocorrelation functions recorded at an angle of 90° .

The micelles of pellet 7 were found to have a hydrodynamic radius of 57 ± 1 nm. No angular variation in the diffusion coefficient was detectable

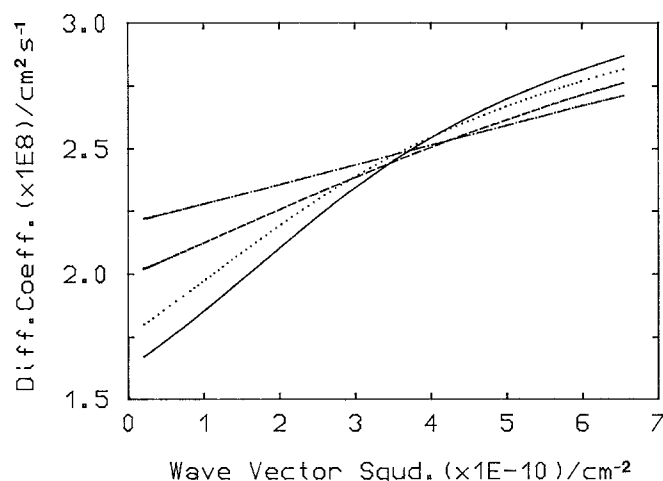


Fig. 5. The apparent diffusion coefficient calculated as a function of k^2 for the distributions of Fig. 2. Again the same symbols as Fig. 2 apply

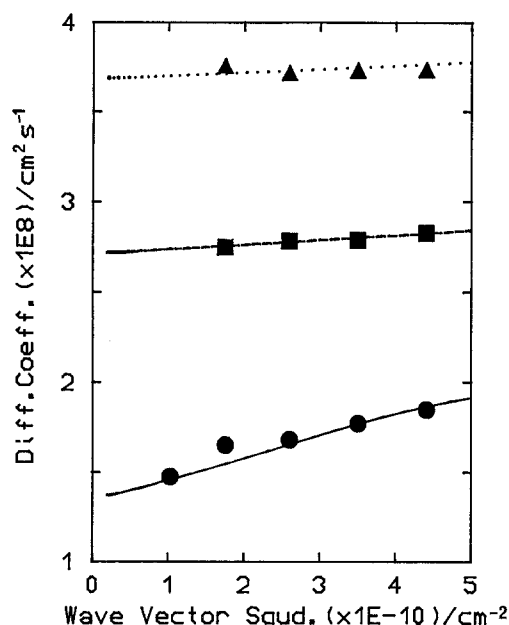


Fig. 6. Experimentally measured diffusion coefficients at different scattering angles for pellets 2 (●), 5 (■), and 7 (▲) together with the predicted angular variation of the calculated diffusion coefficients from 'best-fit' solutions from correlation data. Solutions were selected on the closeness of calculated behaviour to measured D_z vs k^2 plots

for this pellet. The objective in POLY-BAS fitting was thus to generate a solution which predicted a diffusion coefficient value of $3.75 \times 10^{-8} \text{ cm}^2 \text{ s}^{-1}$ at 90° and as little angular variation in D_z as possible. This was achieved with input fitting parameters in the ranges, LS between 70 and 80 nm and DF between 1.4 and 1.6. Outside these ranges the solutions were unsatisfactory, being unable to reproduce the experimental D_z (90°) value and/or its lack of angular variation. The weight fraction distributions shown in Fig. 7 for the parameter values mentioned above and the central distribution selected as the 'best-fit' thus gives some idea of the precision achievable using POLY-BAS for this size of particle. It should be noted that as the particle size increases and the scattering factor becomes more angle dependent, the criteria on which solution selection has been based will operate to narrow the range of permissible solutions and improve greatly on the precision shown for this small-micelle sample.

The stability and reproducibility of the POLY-BAS fitting procedure is demonstrated in Fig. 8 where the weight fraction distributions output from the analysis of three successive autocorrelation runs on a pellet-5 micellar suspension have been derived using the same fitting parameters. The random experimental errors transmit through the inversion process to produce around a 10% variation in the peak amplitude though little variation in its

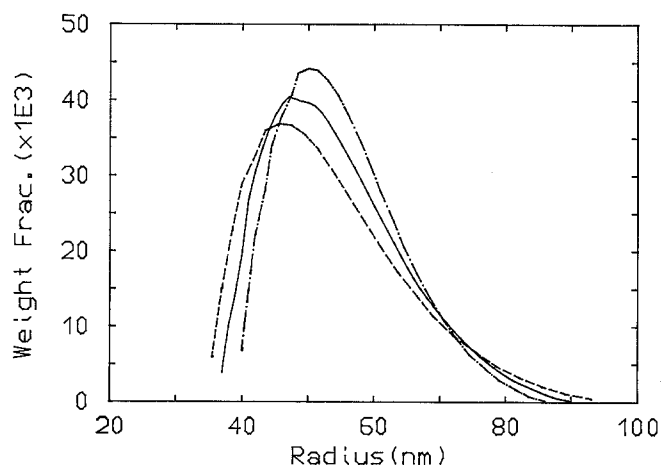


Fig. 7. Weight fraction distributions derived from a single correlation function for a pellet-7 suspension. These illustrate the range of input parameters which lead to solutions still reproducing within experimental error the measured variation (or lack of variation) of D_z vs k^2 for pellet-7 micelles. *Solid line* used LS75, US220, DF1.5 (predicted D_z behaviour shown dotted in Fig. 6); *dashed-dotted* used LS80, US220, DF1.4; *dashed* used LS70, US280, DF1.6

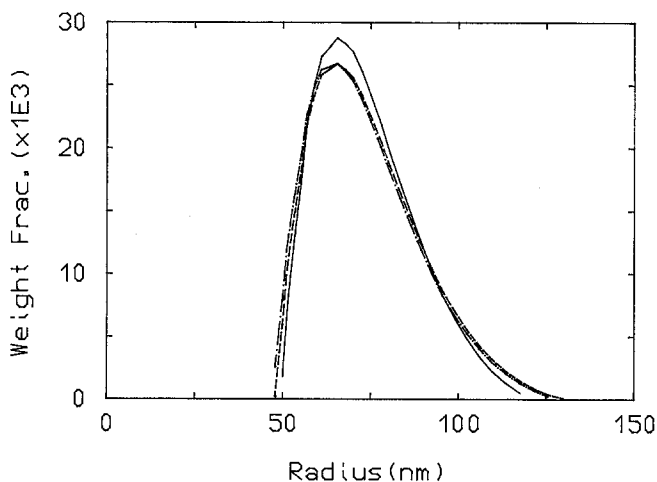


Fig. 8. Three weight fraction distributions derived from three separate correlation functions from a pellet-5 suspension, illustrating reproducibility of technique. All used input parameters LS100, US300, DF1.5

width and position. All three distribution functions drawn in this figure reproduced the measured diffusion coefficients for pellet 5 at all four angles within the experimental error limits (Fig. 6). In this instance, slight variations in the input fitting parameters produced changes in the weight fraction distribution of the same order of magnitude as random experimental variation in the data.

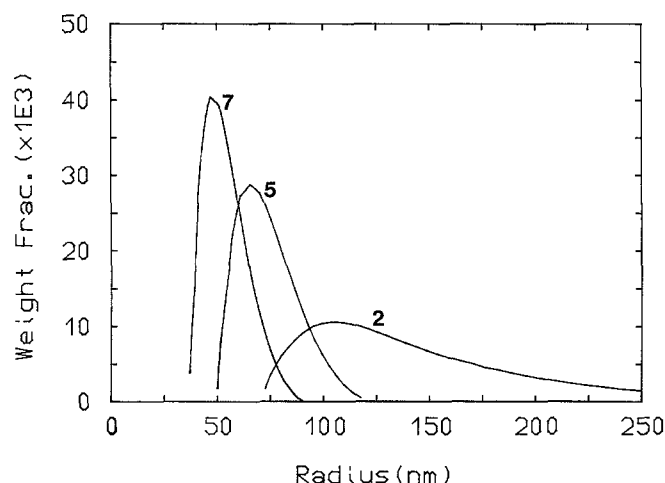


Fig. 9. Weight fraction distributions for pellet-2, -5, and -7 suspensions. These solutions give the 'best-fit' calculated behaviour for D_z vs k^2 compared to measured angular variation as shown in Fig. 6

POLY-BAS is unable to cope with fine structure in $G(D)$ either due to the distributions themselves or to the effects of particle scattering weighting (Pike 1981). Calculated using the RGD approximation, the first minimum in particle scattering factor for 90° scattering occurred around a radius of 230 nm for our systems. As shown in Fig. 9, the weight fraction distribution derived on inversion of a pellet-2 correlation function extended into but little beyond this region. Due to the particle scattering weighting, however, the long tail in this distribution function, much longer than those of pellets 5 and 7, contributed little to the total scattering at 90° . It became increasingly important at smaller angles, however, and overall this distribution reproduced fairly well the experimentally observed angular variation in D_z (Fig. 6).

The centrifugation conditions listed in Table 1 were chosen to produce micellar fractions if not monodisperse, at least with size distributions of acceptably narrow width. As well as demonstrating the aptness of the choice of conditions, the versatility of POLY-BAS in dealing with narrow width distributions over a fairly broad size range has been put to the test. As a further test with a much wider size distribution, autocorrelation functions were recorded over a range of scattering angles between 30° and 105° for dilute suspensions of micelles from the supernatant left after the preparation of pellet 2. This was effectively skim-milk from which the largest micelles had been removed. Cumulants analyses on these autocorrelation functions gave the diffusion coefficients plotted in Fig. 10, shown together with the angular behaviour of D_z predicted by the 'best-fit'

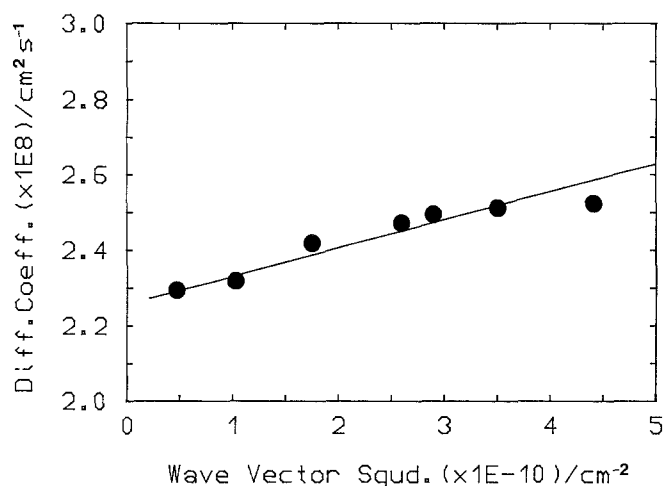


Fig. 10. Experimentally measured diffusion coefficients as a function of k^2 for a suspension of casein micelles from supernatant 2, together with the angular variation predicted (solid line) by a POLY-BAS solution derived from the correlation function measured at 60°

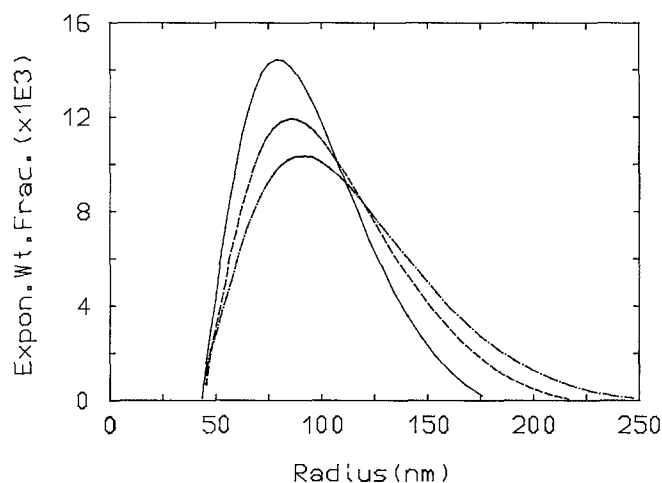


Fig. 11. Exponential weight fraction distributions derived from correlation functions obtained at different angles with a supernatant-2 suspension. All are 'best-fit' solutions giving predicted angular D_z behaviour comparable to that measured. Measuring angles and solutions were as follows 90° solid line, 45° dashed, 30° dashed-dotted

inversion of autocorrelation functions measured at 60° .

Figure 11 shows the 'best-fit' exponential weight fraction distribution satisfying the diffusion coefficient criteria obtained by inverting autocorrelation functions measured at three different scattering angles. The influence of the $P(\theta)$ weighting is clearly seen in the peak shift and apparent transfer of material to larger radius as the angle was decreased. Correcting for the scattering factor weighting and division by R^3 gave the weight fraction distributions of Fig. 12. If the use of the Rayleigh-Gans-Debye

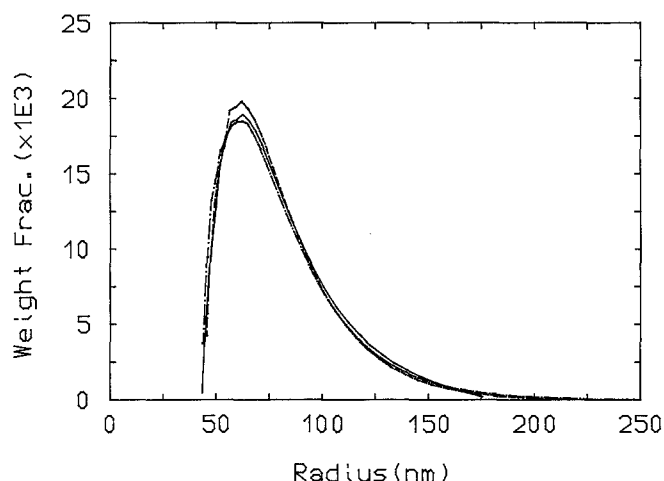


Fig. 12. Weight fraction distributions calculated from the exponential weight fraction distributions of Fig. 11. Same line symbols apply

approximation was invalid, the weight fraction distributions obtained with the different scattering angles would not agree nor would these distributions correctly reproduce the angular dependence of the measured diffusion coefficients.

Attempts to apply POLY-BAS analysis supplemented with the requirements of reproducing observed angular variations of D_z to a suspension of micelles from skim-milk i.e., to determining the entire size distribution and not some portion of it, have not met with complete success. It would be desirable to include the possibility of large micelles of the order of 250–300 nm radius contributing to the scattering. As mentioned previously, the first minimum in the particle scattering function occurs just below this size range at 90° . The inability of POLY-BAS to cope with such oscillations has already been noted. Such fine structure could be avoided by reducing the measuring angle. But with skim-milk micellar suspensions, scattering at low angles tends to be dominated by trace amounts of large diameter fat globules whose total removal presents profound difficulty (Horne 1984). Some other strategy may have to be adopted if inversion of autocorrelation functions is to yield the complete size distribution of native casein micelles.

Acknowledgements. We would like to thank Dr. T. L. Whately, Department of Pharmacy, University of Strathclyde for introducing

us to 'POLY-BAS'. Our thanks are also due to Mrs. C. Davidson for technical assistance.

References

- Bertero M, Pike ER (1983) On the extraction of polydispersity information in photon correlation spectroscopy. In: Schulz-Dubois EO (ed) *Photon correlation techniques in fluid mechanics*. Springer, Berlin Heidelberg New York, pp 298–302
- Cummins HZ, Pike ER (1974) *Photon correlation and light beating spectroscopy*. Plenum Press, New York
- Grabowski EF, Morrison ID (1983) Particle size distributions from analyses of quasi-elastic light-scattering data. In: Dahneke BE (ed) *Measurements of suspended particles by quasi-elastic light-scattering*. Wiley, New York, pp 199–236
- Gulari E, Gulari E, Tsunashima Y, Chu B (1979) Photon correlation spectroscopy of particle distributions. *J Chem Phys* 70: 3965–3972
- Horne DS, Parker TG (1980) The pH sensitivity of the ethanol stability of individual cow milks. *Neth Milk Dairy J* 34: 126–130
- Horne DS (1984) Determination of the size distribution of bovine casein micelles using photon correlation spectroscopy. *J Colloid Interface Sci* 98: 537–548
- Kerker M (1969) *The scattering of light and other electromagnetic radiation*. Academic Press, New York
- McWhirter JG, Pike ER (1978) On the numerical inversion of the Laplace transform and similar Fredholm integral equations of the first kind. *J Phys A: Math Gen* 11: 1729–1745
- Ostrowsky N, Sornette D, Parker P, Pike ER (1981) Exponential sampling method for light scattering polydispersity analysis. *Opt Acta* 28: 1059–1070
- Ostrowsky N, Sornette D (1983) Data reduction in polydisperse diffusion studies. In: Schulz-Dubois EO (ed) *Photon correlation techniques in fluid mechanics*. Springer, Berlin Heidelberg New York, pp 286–297
- Pike ER (1981) The analysis of polydisperse scattering data. In: Chen SH, Chu B, Nossal R (eds) *Scattering techniques applied to supramolecular and non-equilibrium systems*. Plenum Press, New York, pp 179–200
- Pike ER, Watson D, McNeil Watson F (1983) Analysis of polydisperse scattering data II. In: Dahneke BE (ed) *Measurements of suspended particles by quasi-elastic light-scattering*. Wiley, New York, pp 107–128
- Provencher SW (1979) Inverse problems in polymer characterization: direct analysis of polydispersity with photon correlation spectroscopy. *Makromol Chem* 180: 201–209
- Pusey PN, Koppel DE, Schaefer DE, Camerini-Otero RD, Koenig SH (1974) Intensity fluctuation spectroscopy of laser light scattered by solutions of spherical viruses: R17, Q, BSV, PM2 and T7. I. Light-scattering technique. *Biochemistry* 13: 952–960
- Stelzer E, Ruf H, Grell E (1983) Analysis and resolution of polydisperse systems. In: Schulz-Dubois EO (ed) *Photon correlation techniques in fluid mechanics*. Springer, Berlin Heidelberg New York, pp 329–334